A phase insensitive all-optical router based on nonlinear lenslike planar waveguides

Eduardo F. Mateo and Jesús Liñares

Área de Óptica. Departamento de Física Aplicada. Facultade de Física e E. U. deÓptica e Optometría, Universidade de Santiago de Compostela, Campus Sur s/n. E-15782 Santiago de Compostela. Galicia. Spain.

faoptedu@usc.es

Abstract: We present the design of an all-optical router based on the properties of both propagation and interaction of Gaussian beams in lenslike planar guides. Variational results of single co- and counterpropagation are derived and used to design three integrated optical devices, that is, a header extraction device, an optical bistable device and a data routing device, which perform an ultrafast, phase-insensitive and fiber compatible routing operation in the optical domain.

OCIS codes: (190.4390) Nonlinear optics, Integrated optics; (230.1150) All-optical devices; (200.4560) Optical data processing.

References and links

1. G. Stix, "The triumph of light," Scientific American, January (1998).
2. B. Olsson, L. Rau, and J. Blumenthal,"WDM to OTDM multiplexing using an ultrafast all-optical wavelength converter," IEEE Photon. Technol. Lett. **13**, 1905 (2001).
3. J. Blumenthal, B. Olsson, G. Rossi, T. E. Dimmick, L. Rau, M. Masanovic, O. Lavrova, R. Doshi, O. Jerphagnon, J. E. Bowers, V. Kaman, L. A. Coldren, and J. Barton, "All-optical label swapping networks and technologies," J. Lightwave Technol. **18**, 2058 (2000).
4. I. Glesk, K.I. Kang, and P. R. Prucnal, "Ultrafast photonic packet switching with optical control," Opt. Express **1**, 126 (1997).
5. K. H. Park, and T. Mizumoto, "All-optical address extraction for optical routing," Opt. Eng., **38**, 1848 (1999).
6. V. W. S. Chan, K. L. Hall, E. Modiano and K. A. Rauschenbach, "Architectures and technologies for high-speed optical data networks," J. Lightwave Technol. **16**, 2146 (1998).
7. H. J. Lee, J. B. Yoo, V. K. Tsui, and K. H. Fong, "A simple all-optical label detection and swapping technique incorporating a fiber Bragg grating filter," IEEE Photon. Technol. Lett. **13**, 635 (2001).
8. D. Anderson, and M. Lisak, "Bandwidth limits due to incoherent soliton interaction in optical-fiber communication systems," Phys. Rev. A **32**, 2270 (1985).
9. A. E. Kaplan, "Optical bistability that is due to mutual self-action of counterpropagating beams of light," Opt. Lett. **6**, 360 (1981).
10. E. F. Mateo, J. Liñares, and C. Montero, "Intrinsic bistability achieved by transverse modal coupling in a nonlinear integrated device," J. Opt. A: Pure Appl. Opt. **4**, 562 (2002).
11. F. Garzia, C. Sibilia, and M. Bertolotti, "All-optical serial switcher," Opt. Quantum Electron. **32**, 781 (2000).
12. J. H. Marburger, and F. S. Felber, "Theory of a lossless nonlinear Fabry-Perot interferometer," Phys. Rev. A **17**, 335 (1978).
13. R. A. Sammut, C. Pask, and Q. Y. Li, "Theoretical study of spatial solitons in planar waveguides," J. Opt. Soc. Am. B **10**, 485 (1993).
14. R. G. Hunsperger, *Integrated optics: Theory and technology* (Springer-Verlag, Berlin, 1991).
15. E. F. Mateo, and J. Liñares, "All-optical integrated logic gates based on intensity-dependent transverse modal coupling," Opt. Quantum Electron. **35**, 1221 (2003).
16. D. Anderson, "Variational approach to nonlinear pulse propagation in optical fibers," Phys.Rev. A **27**, 3135 (1983).

#6293 - $15.00 US Received 11 January 2005; revised 18 April 2005; accepted 19 April 2005

17. J. Liñares, C. Montero, and D. Sotelo, "Theory and design of an integrated optical sensor based on planar waveguiding lenses," Opt. Commun. **180**, 29 (2000).
18. J. Liñares, M. C. Nistal, "Single local mode propagation though ion-exchanged waveguide elements with quasi-abrupt transitions," Jpn. J. Appl. Phys. **35**, L1596 (1996).
19. M. Desaix, D. Anderson, M. J. and Lisak, "Variational approach to collapse of optical pulses," Opt. Soc. Am. B **8**, 2082 (1991).
20. R. J. Gehr, G. L. Fisher, R. W. and Boyd, "Nonlinear-optical response of porous-glass-based composite materials," J. Opt. Soc. Am. B **14**, 2310 (1997).
21. E. F. Mateo, and J. Liñares, "Third order nonlinear integrated device based on an effective graded-index waveguide for all-optical multistability," Fiber and Int. Optics. To be published (2005).
22. J. Liñares, G. C. Righini, and J. E. Alvarellos,"Modal coupling analysis for integrated optical components in glass and lithium niobate," App. Opt. **31**, 5292 (1992).

1. Introduction

The development and perspectives of the Internet Era have represent, an enormous challenge in the task of giving solutions to the continuous growth of bandwidth requirements in communication networks [1].

In the context of fiber-based optical networks, the all-optical data processing plays a major role for future ultrafast communications schemes where bit-rates up to the Terabit barrier will be necessary; thus, operating at a ultra-high speed requires all-optical devices capable to operate in such a way that the entire optical signal routing, switching, processing and so on, can be made in the optical domain. In OTDM asynchronous packet transmission (for instance the IP protocol), a header is usually added to each data packet carrying information in order to identify the destination of the data; accordingly, the header recognition and separation process as well as the routing of the data packet to a proper output port as a function of the binary value of the header, must be one of the first steps towards routing architectures in the all-optical domain [2, 3].

Results about all-optical routing have been previously reported based on TOADs (Terahertz optical asymmetric demultiplexers) [4], NOMLs (Nonlinear optical mirror loops) [5], logic gates [6] or Bragg gratings [7]; for such a devices, the interference phenomena is present and, in consequence, they show a strong phase-sensitivity as well as a high requirements for coherent interactions between data and/or control signals; moreover, the presence of undesirable factors in long-distance optical transmission such as: depolarization properties of optical fibers, finite coherence time of sources or nonlinear dispersive effects, could make difficult a coherent processing in all-optical networks [8].

In this work we present a new strategy to route optical data packets in a phase-insensitive way. The routing configuration (introduced in section 2) is based on the intensity amplification of the header bits and on the properties of the nonlinear propagation and interactions of optical beams in integrated devices; these devices are composed by nonlinear lenslike waveguides and linear integrated multilenses connected to optical fibers. By means of the variational method, the evolution equations for the parameters of a single Gaussian beam propagation and for co- and counterpropagating Gaussian beams are obtained in a nonlinear lenslike waveguide, which can be made by means of a linear film deposited on a parabolic-shaped curved substrate with third-order nonlinear properties (section 3).

The all-optical routing configuration is realized with: a header extraction integrated device (section 4), an optical bistable device (section 5) and a data routing device (section 6). The principles of operation of these devices are the intensity-dependent trajectory of the optical beams in these structures, due to the inhomogeneous distribution of the nonlinearity, the counterpropagation of optical beams (with a feedback control by means of amplitude filtering based on the modal coupling efficiency)[9, 10], and finally, the incoherent cross-interaction of linear and nonlinear waves. These devices, interconnected by optical fibers, perform a single-bit

#6293 - $15.00 US Received 11 January 2005; revised 18 April 2005; accepted 19 April 2005

all-optical routing operation which sets the basis for a generalized N-bit routing, based on a cascaded architecture of various single-bit routers combined with amplification devices for the header (section 7).

The phase-insensitive character of the proposed routing system allows, on the one hand, an efficient routing operation for wavelength demultiplexed signals (without modifying the device characteristics) and on the other hand, it makes sure the robustness of the device when mechanical and/or thermal instabilities are present. Finally, it must be remarked that the data packet is considered here as a low power signal along the whole routing process and therefore it represents a key advantage over soliton processing devices for all-optical networks [11].

2. Phase-insensitive router: principles of operation

As the specific design of the integrated devices, implementing the whole routing operation, will be detailed later, let us introduce the basis of the proposed phase-insensitive routing mechanism sketched in Fig. 1. The primary aim is to route, in an all-optical way, the data packet onto two

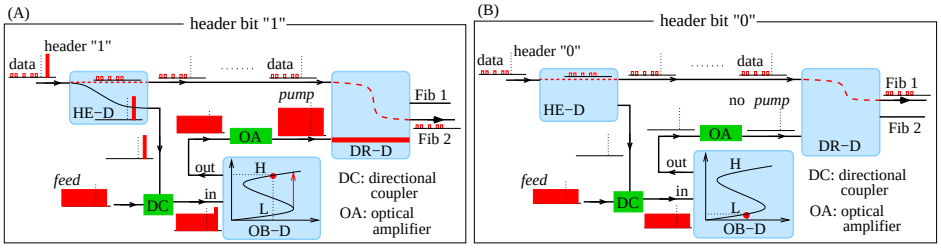

Fig. 1. Sketch of the intensity-dependent routing operation where HE-D represents the Header Extraction Device, OB-D is the Optical Bistable Device and DR-D is the Data Routing Device. In figure (A) is represented the operation under the presence of a 1-valued header bit whereas in figure (B) is represented the operation for a 0-valued header bit.

different optical ports (fiber 1 and 2) depending on the value of the header bit.

Let us start with the routing mechanism for a 1-valued header bit. The first device, labelled as HE-D (*Header Extraction Device*), performs the extraction of the header from data train by means of the power-dependent swing effect experimented by optical beams in the nonlinear lenslike waveguide; therefore, by a suitable design of the waveguide parameters and the initial conditions of the optical beams, the data and header bits can be coupled onto two optical fibers. Next, the header bit is added, by means of a directional coupler, to an OB-D (*Optical Bistable Device*) which is fed with a secondary continuous wave, labelled as *feed*, placing the bistable device on the proper power value (point L); in consequence, when the high power header bit is added, the bistable device jumps to a high transmission state (point H), which is stable due to hysteresis, and it provides an output continuous wave of high power, labelled as *pump*; this pump wave is subsequently amplified by means of an optical fiber amplifier in order to achieve an optimal power value. Finally, both the pump wave and the data packet are injected onto the DR-D (*Data Routing Device*) where the presence of the high intensity pump wave induces a cross-amplitude modulation on the low power data wave, which changes its normal trajectory; obviously, a proper designing of the lenslike parameters and the integrated multilenses will be required to achieve an optimal coupling of the data packet onto the output fiber 2.

Otherwise, when the header bit is 0-valued and accordingly the OB-D has been reseted to its operation point L, the OB-D gives a low output power value, which does not contribute to cross-amplitude modulation in the DR-D and therefore, the injected data packet trajectory does not present any modification on its trajectory in a such a way that they will be coupled onto

#6293 - $15.00 US Received 11 January 2005; revised 18 April 2005; accepted 19 April 2005

fiber 1.

It is important to remark that the three devices involved in the routing operation are designed under the same technology and accordingly the modulation, power values and compatibility with optical fibers are kept unchanged in all the process. For the sake of simplicity, we have just introduced the fundamental mechanism of a single-bit operation with an initial amplified header bit, however, in section 7 is shown how to implement a N-bit routing mechanism with a low power modulation for the header and data bits (more realistic case), by means of a synchronized differential amplification of the header bits and a cascaded configuration of several single-bit routing devices.

3. Propagation and interaction of Gaussian beams in nonlinear lenslike waveguides

The main physical processes involved in the proposed routing device are the nonlinear propagation and nonlinear interactions of optical beams in lenslike nonlinear waveguides. We will derivate in this section, by means of the variational method, the corresponding nonlinear evolution equations containing the following particular cases: the single beam linear and nonlinear propagation, for the design of the HE-D; the coherent counterpropagation of beams, for the design of the OB-D; and incoherent copropagation of beams for the design of the DR-D.

Let us consider a planar step-index waveguide constituted by a nonlinear curved glass substrate of refractive index $n_s^2 + 3\chi_{\mathrm{Re}}^{(3)}\mathscr{E}^2$, where $\chi_{\mathrm{Re}}^{(3)}$ is the real part of the third order nonlinear optical susceptibility and $\mathscr{E}$ is the module of the optical field amplitude. The curved substrate, whose linear refractive index is n_s, is shaped by a parabolic surface represented by the function $f(x) = x^2/l^2$; next, a linear film is deposited on the substrate with a maximum thickness t_0 at $x = 0$; finally, n_c^2 is the cladding index. A sketch of the waveguide is shown in Fig. 2. The linear refractive index profile of the planar waveguide can be written as follows: $n_l^2(x,y) = n_0^2(y) + \Delta n^2(x,y)$, where $n_0^2(y)$ is the linear index profile at $x = 0$ and $\Delta n^2(x,y) = n_s^2 - n_f^2$ for $0 \le y \le f(x)$, represents the index perturbation due the substrate curvature; finally, the nonlinearity distribution is characterized by $\chi_{\mathrm{Re}}^{(3)}(x,y) = \chi_{\mathrm{Re}}^{(3)}$ for $-\infty \le y \le f(x)$.

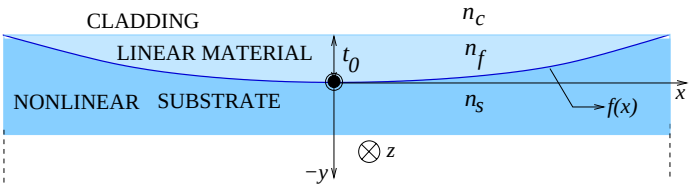

Fig. 2. Transverse view of the waveguide.

It is wellknown that the real vector amplitude of the total optical field $\vec{\mathscr{E}}$ satisfies the following scalar equation:

$$\nabla^2\vec{\mathscr{E}}(\vec{r},t) = \mu_0\frac{\partial^2}{\partial t^2}\left[\varepsilon_0 n_l^2(x,y) + 3\varepsilon_0\chi_{\mathrm{Re}}^{(3)}(x,y)\mathscr{E}^2\right]\vec{\mathscr{E}}. \tag{1}$$

Now, let us consider a set of two TE waves with central frequency ω_0 and unperturbed propagation constants β_1 and β_2, that is,

$$\mathscr{E}(x,y,z,t) = \frac{1}{2}\varphi(y)[\psi_1(x,z)\exp(\mathrm{i}\beta_1 z) + \psi_2(x,z)\exp(\mathrm{i}\beta_2 z)]\exp(-\mathrm{i}\omega_0 t) + cc. \tag{2}$$

where $\beta_1 = \beta_2 = \beta_0$ for the copropagating case and $\beta_2 = -\beta_1$ for the counterpropagating case; $\varphi(y)$ is the unperturbed normalized linear amplitude of the fundamental mode, that is,

#6293 - $15.00 US Received 11 January 2005; revised 18 April 2005; accepted 19 April 2005

($\int \varphi^* \varphi \mathrm{d}y = 1$); and $\psi_\alpha(x,z)$ (with $\alpha = 1,2$) are the z-slowly varying nonlinear envelopes of the beams. This factorization is made under the assumption of a negligible nonlinear effect on the modal amplitude (linear modal amplitude assumption).

For the case of incoherently interacting copropagating beams [8], and coherent counterpropagation of parallel polarized beams [12], the derivation of the propagation equations for the nonlinear envelopes ψ_α is made up by considering only the terms synchronized with the propagation constants β_1 and β_2, after inserting Eq. (2) into Eq. (1), and by performing a z-spatial averaging. For the counterpropagating case, there will be terms oscillating with $\pm 3\beta_0$ which vanish after a z-spatial averaging; likewise, in the case of incoherent copropagation, there will be a beams superposition with random phases, therefore only the terms corresponding with the sum of the beam intensities are conserved. In short, by considering the above assumptions, and by taking into account the expression of the linear index profile, we obtain, after multiplying by $\varphi^*(y)$ and integrating along the y-direction [13], the following expressions for $\psi_\alpha(x,z)$,

$$\begin{aligned} &2\mathrm{i}\beta_\alpha \frac{\partial \psi_\alpha}{\partial z} + \frac{\partial^2 \psi_\alpha}{\partial x^2} + k^2 \left[\int \Delta n(x,y) \varphi^2 \mathrm{d}y \right] \psi_\alpha + \\ &\frac{3}{4} k^2 \left[\int \chi^{(3)}_{\mathrm{Re}}(x,y) \varphi^4 \mathrm{d}y \right] (|\psi_\alpha|^2 + J|\psi_{3-\alpha}|^2) \psi_\alpha = 0, \end{aligned} \tag{3}$$

with $J = 0$ for a single-beam propagation, $J = 1$ for the copropagating case and $J = 2$ for the counterpropagating one.

The integrals of Eq. (3) can be solved by taking into account the perturbative condition ($l >> x$), as it is shown in reference [15], and by taking into account the general expression for the fundamental mode of a step-index planar waveguide, which can be found, for instance, in reference [14]. Accordingly, the above equations can be rewritten as follows,

$$2\mathrm{i}\beta_\alpha \frac{\partial \psi_\alpha}{\partial z} + \frac{\partial^2 \psi_\alpha}{\partial x^2} - G^2 x^2 \psi_\alpha + k^2 \tilde{n}_{k0} (1 + Q^2 x^2)(|\psi_\alpha|^2 + J|\psi_{3-\alpha}|^2) \psi_\alpha = 0, \tag{4}$$

where β_0 is the solution of the dispersion equation for the step-index waveguide. Moreover, G, Q and $\tilde{n}_0$, which depend on the modal parameters ξ_s (p in the notation of reference [14]) and φ_0 (modal amplitude value in $y = 0$), take the following values: $G^2 = k^2(n_f^2 - n_s^2)\varphi_0^2/l^2$, $\tilde{n}_{k0} = 3\chi^{(3)}_{Re}\varphi_0^4/16\xi_s$ and $Q^2 = 4\xi_s/l^2$. The G-factor can be regarded as a linear (effective) gradient index parameter (linear lenslike behaviour) whereas the Q-factor is an effective gradient nonlinear index parameter (power-dependent lenslike behaviour).

By following the variational formalism [10, 16] let us choose a Gaussian multiparametric trial function in order to solve Eq. (4), that is,

$$\psi_\alpha(x,z) = E_{0\alpha} \exp\left[-\frac{(x - x_\alpha)^2}{a^2 w_\alpha^2} \right] \exp\left[\mathrm{i}\beta_\alpha \rho_\alpha (x - x_\alpha)^2 + \mathrm{i} V_\alpha (x - x_\alpha) \right]. \tag{5}$$

The four z-dependent parameters for each envelope are: the normalized beam widths $w_\alpha(z)$, the inverse curvature radius $\rho_\alpha(z)$, the beam peak position $x_\alpha(z)$ and the transverse local wave number $V_\alpha(z)$; a is the initial beam width, therefore $w_\alpha(z=0) = 1$, and $E_{0\alpha}$ is the maximum field amplitude.

After a long but straightforward calculations, the following coupled equations for the relevant Gaussian parameters are obtained:

$$\begin{aligned} &\frac{\mathrm{d}^2 w_\alpha}{\mathrm{d}\tau^2} - \frac{1}{w_\alpha^3} + g w_\alpha + \frac{1}{2} p_\alpha \frac{1}{w_\alpha^2} \left(1 - q w_\alpha^2 + Q^2 x_\alpha^2\right) + \sqrt{2} J p_{3-\alpha} \frac{1}{w_\alpha^2} \times \\ &\left(1 + \frac{w_{3-\alpha}^2}{w_\alpha^2} \right)^{-3/2} (K_{0\alpha} - q K_{1\alpha} + Q^2 K_{2\alpha}) \exp\left[\frac{-2(x_\alpha - x_{3-\alpha})^2}{a^2 w_\alpha^2 + a^2 w_{3-\alpha}^2} \right] = 0, \end{aligned} \tag{6}$$

#6293 - $15.00 US Received 11 January 2005; revised 18 April 2005; accepted 19 April 2005

$$\frac{\mathrm{d}^2 x_\alpha}{\mathrm{d}\tau^2} + g x_\alpha - 2 p_\alpha q x_\alpha \frac{1}{w_\alpha} + \frac{J}{\sqrt{2}} p_{3-\alpha}(D_{0\alpha} - q D_{1\alpha}) \exp\left[\frac{-2(x_\alpha - x_{3-\alpha})^2}{a^2 w_\alpha^2 + a^2 w_{3-\alpha}^2}\right] = 0, \quad (7)$$

$$V_\alpha = \beta_\alpha \frac{\mathrm{d}x_\alpha}{\mathrm{d}\tau}, \quad (8)$$

where $\tau = 2z/\beta_\alpha a^2$, $g = \frac{1}{4}G^2 a^4$, $q = \frac{1}{8}Q^2 a^2$, $p_\alpha = k^2 \tilde{n}_{k0} E_{0\alpha}^2 a^2 / 2\sqrt{2}$ (note that p_α is a parameter which is proportional to the power of the beams), and

$$\begin{aligned} K_{0\alpha} &= 1 - \frac{4(x_\alpha - x_{3-\alpha})^2}{a^2 w_\alpha^2 + a^2 w_{3-\alpha}^2}, \qquad K_{1\alpha} = 2w_{3-\alpha}^2 - 3\frac{w_\alpha^2 w_{3-\alpha}^2}{w_\alpha^2 + w_{3-\alpha}^2}, \\ K_{2\alpha} &= -4\frac{x_{3-\alpha}(w_\alpha^2 x_{3-\alpha} + w_{3-\alpha}^2 x_\alpha)}{w_\alpha^2 + w_{3-\alpha}^2} + 4\frac{(w_\alpha^2 x_{3-\alpha} + w_{3-\alpha}^2 x_\alpha)^2 (x_\alpha - x_{3-\alpha})^2}{a^2 (w_\alpha^2 + w_{3-\alpha}^2)^3} \\ &+ 5\frac{(w_\alpha^2 x_{3-\alpha} + w_{3-\alpha}^2 x_\alpha) + w_\alpha^2 w_{3-\alpha}^2 (x_\alpha - x_{3-\alpha})^2}{(w_\alpha^2 + w_{3-\alpha}^2)^2}. \end{aligned} \quad (9)$$

$$\begin{aligned} D_{0\alpha} &= \frac{(x_\alpha - x_{3-\alpha})}{(w_\alpha^2 + w_{3-\alpha}^2)^{3/2}}, \qquad D_{1\alpha} = 8\frac{w_{3-\alpha}^2 (w_\alpha^2 x_{3-\alpha} + w_{3-\alpha}^2 x_\alpha)}{(w_\alpha^2 + w_{3-\alpha}^2)^{5/2}} \\ &- 4\frac{(x_\alpha - x_{3-\alpha})}{(w_\alpha^2 + w_{3-\alpha}^2)^{5/2}} - 4\frac{(w_\alpha^2 x_{3-\alpha} + w_{3-\alpha}^2 x_\alpha)^2 (x_\alpha - x_{3-\alpha})}{a^2 (w_\alpha^2 + w_{3-\alpha}^2)^{7/2}}. \end{aligned} \quad (10)$$

Let us describe briefly the main effects involved in the light propagation inside the structure sketched in Fig.(2). As expected from Eq. (6) the $g(G)$-factor induces a linear lenslike effect depending on the linear substrate-film index difference and the curvature of the parabolic interface; moreover, the global self-focusing effect is modulated by the Gaussian intensity distribution depending on the power of the beam p_α. The $Q(q)$-factor involves a double effect: by one hand, it compensates the linear gradient effect due the reduction of the index difference between the film and the substrate (since the index of the substrate is increased with the intensity), and by the other hand, it modulates the self-focusing effect as a function of the peak displacement increasing its influence in regions where the field is more present in the substrate. According to the first effect, the oscillatory behaviour of the beam peak displacement, which is induced by a gradient index distribution (swing effect), is in turn modulated as a function of the beam intensity/power (as Eq. (7) shows), and in consequence the period of oscillation is modified. This property is one of the key results of this work (as it will be shown in the HE-D design) since it does not take place in usual nonlinear lenses, where the focusing and/or swing properties are intensity-independent.

4. Design of the header extraction device

We will design an all-optical planar waveguide header recognizer, based on the commented power dependence of the period of the swing of the beam. The device will operate with two different power states, that is, a low power state (data packet) and a high power state (header bit); the design of the device must verify that the beams corresponding to these states be well spatially-resolved to achieve an optimal output coupling onto two different optical fibers. It is assumed that the low power state will undergo a linear propagation, that is $p \sim 0$; and the high power state will be chosen as a quasi-self-trapping state, that is, a state where the Gaussian beam presents small variations of its width around the initial value.

In Fig. 3 it is shown a sketch of the integrated device, where integrated multilenses are placed at the beginning and at the end of the nonlinear waveguide; each multilens can be implemented by waveguiding integrated lenses [17, 18] (see appendix A) and they must be designed in

#6293 - $15.00 US Received 11 January 2005; revised 18 April 2005; accepted 19 April 2005

such a way that it expands/compresses the Gaussian beam along the x-direction from/to the input/output by means of optical fibers in a such a way that it preserves the linear modal amplitude assumption [10] and allows to obtain the optimal value of the initial beam width, as it will be described in detail later.

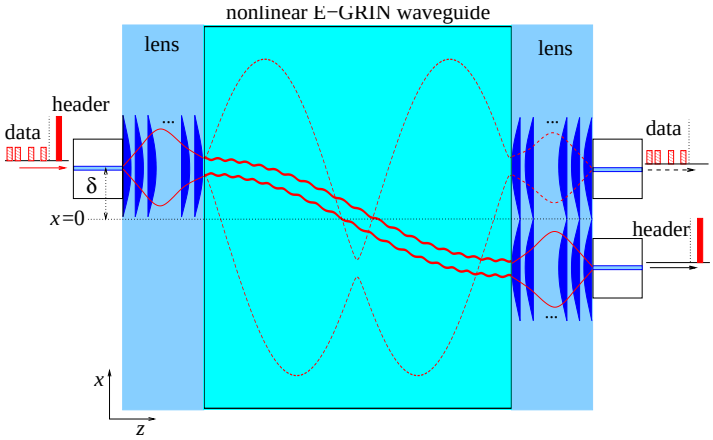

Fig. 3. Top view of the header extraction device where the variational evolution of the header (solid) and data (dashed) Gaussian beam widths are shown.

The variational propagation equations for a single beam are derived by choosing $p_2 = 0$ in Eqs. (6) and (7); thus by denoting with (w_h, x_h) the parameters of the header Gaussian beam with power $p_1 = p_h$, we obtain the following evolution equations:

$$\frac{\mathrm{d}^2 w_h}{\mathrm{d}\tau^2} - \frac{1}{w_h^3} + g w_h + \frac{1}{2} p_h \frac{1}{w_h^2}\left(1 - q w_h^2 + Q^2 x_h^2\right) = 0, \tag{11}$$

$$\frac{\mathrm{d}^2 x_h}{\mathrm{d}\tau^2} + g x_h - 2pq x_h \frac{1}{w_h} = 0. \tag{12}$$

On the other hand, the evolution equations for the data wave (w_d, x_d) are derived from Eqs. (6) and (7) by considering a linear propagation of the data Gaussian beam ($p_1 = p_d << 1$) and again $p_2 = 0$, that is,

$$\frac{\mathrm{d}^2 w_d}{\mathrm{d}\tau^2} - \frac{1}{w_d^3} + g w_d = 0, \tag{13}$$

$$\frac{\mathrm{d}^2 x_d}{\mathrm{d}\tau^2} + g x_d = 0. \tag{14}$$

For the header Gaussian beam, the above-mentioned nonlinear quasi-self-trapping state is obtained as follows: if we consider a non-displaced Gaussian beam ($\delta = 0$), we can calculate the value of power p_{st} for self-trapping: $w_h(p_{st}, x_h = 0, z) = 1$, from Eq. (11) (see for example [16, 19]), that is,

$$p_{st} = \frac{2(1-g)}{1-q} = \frac{16 - 4G^2 a^4}{8 - Q^2 a^2}. \tag{15}$$

When this power value is used for displaced Gaussian beams ($\delta \neq 0$) a quasi-selftrapping beam is obtained such as it is showed in Fig.3 (solid line).

By launching both the data and header Gaussian beams with an initial displacement δ, oscillating trajectories (swing effect) are obtained, and therefore spatial periods of oscillation can

#6293 - $15.00 US
Received 11 January 2005; revised 18 April 2005; accepted 19 April 2005

be defined for the corresponding trajectories, that is, Λ_d for the data Gaussian beam (obtained from Eq. (14)) and Λ_h for the header Gaussian beam (obtained from Eq. (12) with p_{st}). A simple condition for achieving a maximum spatial separation between the beams is obtained under the following condition: $\Lambda_h = 2\Lambda_l$ (see Fig.3). Now, we must calculate these periods and, as the $g(G)$ and $q(Q)$ factors depend on the waveguide parameters, the first step will be to obtain a proper design of the waveguide in order to enlarge the nonlinear contribution to the swing effect and so increase the difference between Λ_h and Λ_l; for that, we have considered a substrate formed by a porous nonlinear glass [20] and a film formed by an organic material with the following characteristics: $n_s = 1.500$ and $n_f = 1.540$ at $\lambda = 0.532$ μm, $n_c = 1.000$, $t_0 = 2.40$ μm and $l = 400.0$ μm$^{1/2}$; moreover, we have taken an initial peak displacement $\delta = 40\mu$m.

It can be easily derived from Eq. (14) that the peak trajectory of the data beam is given by the solution $x_d(\tau) = \delta\cos(g^{1/2}\tau)$, therefore the linear period is

$$\Lambda_l = \frac{2\pi}{g^{1/2}} = \frac{4\pi}{Ga^2}. \tag{16}$$

On the other hand, the initial beam width a of the beams is taken as a designing parameter; thus, from the numerical solutions of Eqs. (11) and (12), and by taking into account Eqs. (15) and the expression (16), we can find the value of a which fulfills the condition for the swing periods. The numerical result was $a = 6.87$ μm and therefore with the following factors $g = 3.40\times10^{-3}$, $q = 5.82\times10^{-4}$ and $p_{st} = 1.994$.

In Figs. 4-(a) and (b) it is shown the evolution of the Gaussian widths of the linear and quasi-self-trapped beams, respectively.

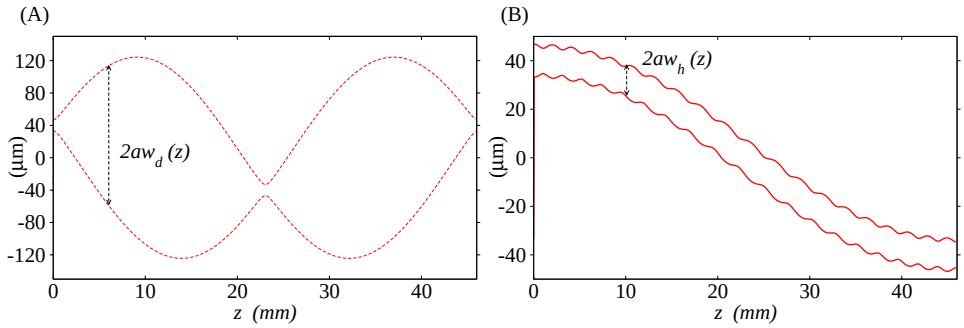

Fig. 4. Variational results for the data (A) and header (B) beam propagation.

5. Design of the optical bistable device

Intrinsic *all-optical* bistability by nonlinear amplitude modulation (therefore it is insensitive to nonlinear phase modulation) is based on the mutual nonlinear interaction of two counterpropagating beams. In our case, the nonlinear amplitude modulation is due, on the one hand, to the nonlinear changes of the effective index of a planar waveguide, and on the other hand, to linear amplitude transformations obtained by transverse modal coupling between an optical fiber mode and the nonlinear Gaussian beams. Likewise, the bistable behaviour for input powers p_{in}, is characterized by a low and high transmission states of optical power at the output of the device (p_{out}), which are joined by an hysteresis loop in the plane $p_{in} - p_{out}$.

In Fig. 5 it is shown the integrated device proposed for optical bistability. The device is made up by an nonlinear planar waveguide with the same characteristics that the one designed for the HE-D unless the curvature of the of the substrate-film interface, which, for the sake of

#6293 - $15.00 US Received 11 January 2005; revised 18 April 2005; accepted 19 April 2005

simplicity, has been chosen as planar ($l >>$) (otherwise, it could arise undesired multistable loops [21]); in addition, two linear subsystems (input and feedback ones) formed by integrated-lenses and optical single-mode fibers are included. A reflective element, with reflectance R, is incorporated to the feedback subsystem, in order to obtain the optical counterpropagation. Finally, the regressive (feedback) beam is collected by the input lens providing, by means of a directional coupler, the output power value.

The input subsystem transforms the modal amplitude of the input fiber into an elliptical one, expanding by a first integrated multilens the optical field along the *x*-direction; next, after the beam propagation along the nonlinear planar waveguide, the light is coupled onto the optical fiber, with a reflective end, by means of a second integrated multilens, which is specularly identical to the input one. At low power values the optical beam will arrive diffracted to the second multilens (plane z_2) and, as it performs the inverse beam transformation of the first multilens, a diffracted beam will be coupled inefficiently onto the optical fiber (as it is shown in Fig. 5, which provides a poor feedback and consequently a poor output transmission. As the optical power is increased the beam tends to a self-confinement regime; in this case, the second multilens will couple the nonlinear envelope to the optical fiber in a more efficient way, which provides an intense reflected beam and therefore, a high transmission output. Under this condition, the cross-action of the nonlinear counterpropagating beams creates an state of *waves-guiding-waves* which keeps a quasi-self-trapped state even when the input power is reduced, making sure a high transmission behaviour, within an hysteresis loop, such as it is required in an optical bistable behaviour.

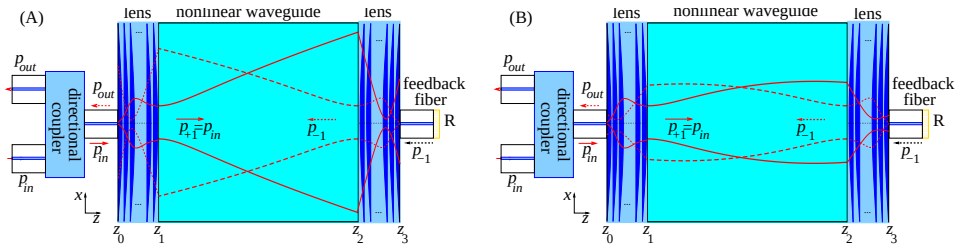

Fig. 5. Sketch of the bistable device showing the propagation behaviour of the counterpropagating beams in cases of low (A) and high (B) transmission output.

Let us denote as $p_{+1} \equiv p_{in}$ and w_{+1} the power parameter and beam width of the forward beam, and p_{-1} and w_{-1} the power parameter and the width of the backward (feedback) beam (see Fig. 5). As it was mentioned above, for optical bistability we will consider an homogeneous planar waveguide ($l >>$) and in consequence $g = Q = q = 0$; likewise, collinear beams are assumed, where $x_{+1} = x_{-1} = 0.0$. Under such assumptions, the variational equations (6) for the counterpropagating beams ($J = 2$) are now given, with the new notation, by,

$$\frac{\mathrm{d}^2 w_{+1}}{\mathrm{d}\tau^2} - \frac{1}{w_{+1}^3} + \frac{1}{2} p_{+1} \frac{1}{w_{+1}^2} + 2\sqrt{2} p_{-1} \frac{1}{w_{+1}^2} \left(1 + \frac{w_{-1}^2}{w_{+1}^2}\right)^{-3/2} = 0, \tag{17}$$

$$\frac{\mathrm{d}^2 w_{-1}}{\mathrm{d}\tau^2} - \frac{1}{w_{-1}^3} + \frac{1}{2} p_{-1} \frac{1}{w_{-1}^2} + 2\sqrt{2} p_{+1} \frac{1}{w_{-1}^2} \left(1 + \frac{w_{+1}^2}{w_{-1}^2}\right)^{-3/2} = 0. \tag{18}$$

It can be demonstrated, by following the calculus from reference [10], that the transverse coupling efficiency between the forward beam and the fiber modal amplitude at the plane z_3, is

#6293 - $15.00 US
Received 11 January 2005; revised 18 April 2005; accepted 19 April 2005

given, as a function of the forward beam width at plane z_2, by the following expression,

$$\eta_3(p_{+1}, p_{-1}) = \frac{2w_{+1}(z_2, p_{+1}, p_{-1})}{1 + w_{+1}^2(z_2, p_{+1}, p_{-1})}, \tag{19}$$

where the value of w_{+1} at z_2 is given by Eqs. (17) and (18) after a propagation distance $|z_2 - z_1|$. Next, the power value of the backward beam is calculated by taking into account the transverse modal coupling and the reflection onto the output fiber, that is,

$$p_{-1} = \eta_3(p_{+1}, p_{-1}) R p_{+1}. \tag{20}$$

Finally, the output power is given by the product of the backward power p_{-1} and the transverse modal coupling of the backward beam at the plane Z_0, that is,

$$\eta_0(p_{-1}, p_{+1}) = \frac{2w_{-1}(z_1, p_{-1}, p_{+1})}{1 + w_{-1}^2(z_1, p_{-1}, p_{+1})}, \tag{21}$$

where,

$$p_{out} = p_{-1}\eta_0(p_{+1}, p_{-1}). \tag{22}$$

In short, we must solve the equations system given by Eqs. (17) and (18) with the implicit condition given by Eq. (20), in order to obtain the final $p_{in} - p_{out}$ results. For that, we solve the equations system for the beam widths, starting from an initial value of p_{-1}, and iteratively we find the value or values (since there will be multivalued point due to the bistability) of p_{-1} which fulfills the condition (20) for a given value p_{in}; iteration is based on the searching of roots of Eq. (20).

In Fig. 6 it is shown the result of the bistable calculus, for a reflectivity of $R = 1.0$ and a propagation distance of $|z_2 - z_1| = 2.1$ mm. The propagation behaviour of the bistable operation (points A and B), it is shown in Figs. 5-A and -B respectively, extracted from the solutions of the equations (17) and (18).

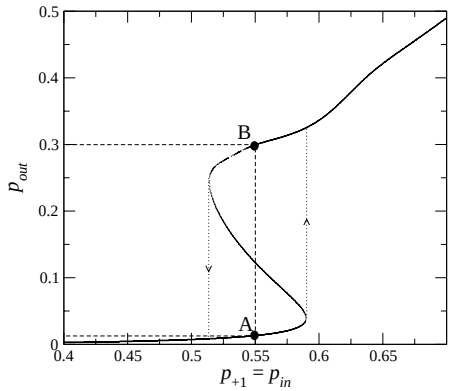

Fig. 6. Optical bistability plot showing the bi-valued points for routing operation at $p_{in} = 0.55$, where A is the output power value for a header bit "0", and B is for the header value "1".

As it is shown in the bistability plot, we must fix the power of the bistability feed input (*feed* in Fig. 1) equal to $p_{in} = p_{feed} = 0.55$, therefore, when the header bit is added to the bistable feed power, the output switches to a high transmission state providing an output power value (in normalized units) $p_{out} = 0.3$. This value must be amplified since (as we will see later), the pump

#6293 - $15.00 US Received 11 January 2005; revised 18 April 2005; accepted 19 April 2005

signal for the DR-D must fulfill the quasi-self-trapping condition ($p_{st} \sim 2$) in the same way that in the header extraction device. It is important to stress here that the the power parameters p depend on the waveguide structure via the averaged third order susceptibility; in this way, we have considered the same waveguide parameters and material configuration which allows us to talk in terms of power parameters instead of real power values.

6. Design of the data routing device

We will perform the design of the device devoted to the derivation of the data as a function of the bistable output, which in turn, depends on the header bit value. The main task is to achieve an optimal coupling of the data packet wave onto two different optical fibers (output channels) depending on the presence or absence of the pump wave generated by the header bit. The pump wave, as in the HE-D, is propagated in a quasi-self-trapping state and it will induce changes on the refractive index, due third order nonlinearity, which will affect on the data packet wave by modifying its beam width and peak trajectory. The most important aim is to avoid the cross-talk between the output channels, that is, the presence of part of the data wave in its non-corresponding optical fiber; therefore, the coupling efficiency of the data packet in its corresponding channel must by sufficiently high and moreover, a fully negligible coupling efficiency in its non-corresponding optical fiber must be achieved. On the other hand, the pump wave must not increase in a relevant way the data transmission power in order the preserve the data power values in a linear regime. This requirement is important for a cascaded system where the output signals are used as input signals of new devices.

Let us start by denoting the Gaussian parameters p, w, x and V with two subindexes where the first one is related to the type of wave pump (p) or data (d) and the second one is related to the state of the device that is, pump off (header 0) and pump on (header 1) that is, we have the following cases: data wave (pump off) $(p_{d0}, w_{d0}, x_{d0}, V_{d0})$; data wave (pump on) $(p_{d1}, w_{d1}, x_{d1}, V_{d1})$ and pump wave $(p_{p1}, w_{p1}, x_{p1}, V_{p1})$.

By considering again, as in section 4, that the power of the data sufficiently low for making sure a linear regime, that is, $p_{d0} = p_{d1} \sim 0$, let us rewrite the evolution equations (6) and (7) for the data and pump beams for both the case of absence (header bit 0) and presence (header bit 1) of pump. For the first case we have that,

$$\frac{\mathrm{d}^2 w_{d0}}{\mathrm{d}\tau^2} - \frac{1}{w_{d0}^3} + g w_{d0} = 0, \quad \frac{\mathrm{d}^2 x_{d0}}{\mathrm{d}\tau^2} + g x_{d0} = 0, \quad V_{d0} = \beta_0 \frac{\mathrm{d}x_{d0}}{\mathrm{d}\tau}. \tag{23}$$

For the second case,

$$\begin{aligned} &\frac{\mathrm{d}^2 w_{p1}}{\mathrm{d}\tau^2} - \frac{1}{w_{p1}^3} + g w_{p1} + \frac{1}{2} p_{p1} \frac{1}{w_{p1}^2} \left(1 - q w_{p1}^2 + Q^2 x_{p1}^2\right), \\ &\frac{\mathrm{d}^2 x_{p1}}{\mathrm{d}\tau^2} + g x_{p1} - 2 p_{p1} q x_{p1} \frac{1}{w_{p1}} = 0, \qquad V_{p1} = \beta_0 \frac{\mathrm{d}x_{p1}}{\mathrm{d}\tau}. \end{aligned} \tag{24}$$

Moreover, the evolution equations for the data wave width in the presence of pump are given by,

$$\begin{aligned} &\frac{\mathrm{d}^2 w_{d1}}{\mathrm{d}\tau^2} - \frac{1}{w_{d1}^3} + g w_{d1} + \\ &+ \sqrt{2} p_{p1} \frac{1}{w_{d1}^2} \left(1 + \frac{w_{p1}^2}{w_{d1}^2}\right)^{-3/2} (K_0 + q K_1 - Q K_2) \exp\left[\frac{-2(x_{d1} - x_{p1})^2}{a^2 w_{d1}^2 + a^2 w_{p1}^2}\right] = 0, \end{aligned} \tag{25}$$

#6293 - $15.00 US Received 11 January 2005; revised 18 April 2005; accepted 19 April 2005

where the values of the K-functions are given by Eqs. (9) with the proper notation. Finally, the peak displacement and the wave number of data beam in the presence of pump are given by,

$$\frac{\mathrm{d}^2 x_{d1}}{\mathrm{d}\tau^2} + g x_{d1} + \frac{1}{\sqrt{2}} p_{p1}(D_0 - qD_1) \exp\left[\frac{-2(x_{d1}-x_{p1})^2}{a^2 w_{d1}^2 + a^2 w_{p1}^2}\right] = 0,$$
$$V_{d1} = \beta_0 \frac{\mathrm{d}x_{d1}}{\mathrm{d}\tau}, \tag{26}$$

where the functions D_0 and D_1 are given by Eqs. (10).

Once the evolution equations for the relevant parameters are given (the effect of the curvature radius on the transverse modal coupling is negligible), let us perform the design of the device in order to achieve an optimal coupling of the data onto the output optical fibers depending on the presence or absence of the pump wave. We will consider the characteristics of the nonlinear waveguide identical to those ones chosen for the HE-D in order to keep invariant the power values of the system; likewise, the pump wave will be considered in a quasi-self-trapping regime, that is, $w_{p1} \sim 1$. First let us advance the results on the design and the structure of the device and later we will present the calculations. In Figs. 7 are shown both the device and the variational propagation of the two states under a top view of the beam widths (taken as 1/e of the peak amplitudes).

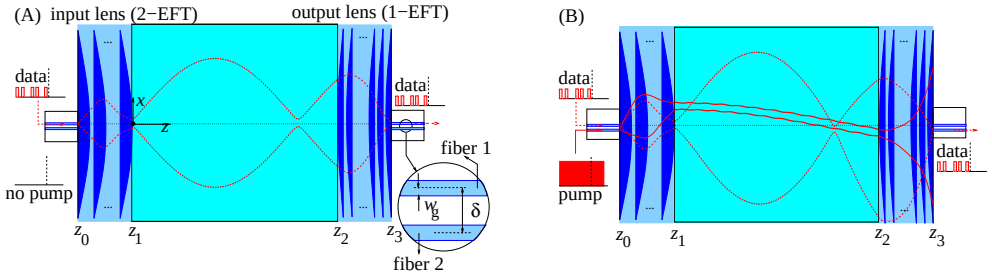

Fig. 7. Integrated device performing the data routing under the absence (A) and presence (B) of the pump wave. The variational evolution of the pump (dashed) and data (solid) are shown for each case.

The input lens is designed, as in the previous devices, in order to expand the beams along the x direction to an initial Gaussian beam width of $a = 6.87$. The input fibers are separated a distance $\delta = 5w_g$, where w_g is the modal radius of the fiber mode, which is assumed to be equal to the modal radius of the modal amplitude of the planar waveguide which takes the value, $w_g = 1.33$ μm; the distance δ is chosen as short as possible to maximize the interaction between the pump and data waves in an also short propagation distances $(z_2 - z_1)$; moreover, the input fibers are placed in such a way that the input data channel is at $x = 0$, that is $x_{d0}(z_1) = x_{d1}(z_1) = 0$ and the pump channel is at $x = -\delta$; thus, the input multilens, designed with 2 EFT modules (see appendix A), shifts the pump wave a value $x_{p1}(z_1) = B_2\delta/B_1 = 5a$ at the plane z_1 (see Fig. 7-(B)), as they show the multilenses transformation laws given by Eqs. (A.5).

It is clear, from the above assumptions that the data wave in the absence of pump will not experiment any peak displacement since it is launched along the symmetry z-axis of the substrate-film curved interface; therefore, it will couple onto an output optical fiber at $x = 0$; however, when the pump wave is present, the data wave will interact with the high power pump wave modifying its propagation, that is, the data beam will undergo a peak displacement; moreover, as in the HE-D, the pump wave will experiment a swing effect due to its initial peak shifting respect to $x = 0$.

#6293 - $15.00 US
Received 11 January 2005; revised 18 April 2005; accepted 19 April 2005

We start the calculation by choosing a separation of the output fibers equal to δ; therefore, in the presence of pump, the data wave will be optimally coupled onto fiber 2 if the following conditions are fulfilled at plane z_3, that is

$$aw_{d1}(z_3) = w_g, \quad x_{d1}(z_3) = -\delta. \tag{27}$$

For the sake of simplicity we have not imposed any restriction on the wave number V_{d1} at the plane z_3.

Now, by taking into account the transformation relationships for an output multilens with one EFT-module, and by considering the above expressions, we have the following expressions for the values of the Gaussian parameters of the data wave at the plane z_2, that is,

$$aw_{d1}(z_2) = \frac{2B}{k}\frac{1}{w_g}, \quad V_{d1}(z_2) = \frac{k\delta}{B}. \tag{28}$$

Finally, by taking the product of the above expressions, the Gaussian beam parameters of the data wave under the presence of the pump wave and the B parameter of the output multilens must fulfill the following condition

$$aw_{d1}(z_2)V_{d1}(z_2) = -\frac{2\delta}{w_g} = -10, \qquad B/k = \frac{1}{2}aw_{d1}(z_2)w_g. \tag{29}$$

It is important to stress that the Gaussian parameters at the plane z_2 for both the pump wave and the data wave in the absence of pump, are now completely determined by the condition (29) since it will fix both the length of the nonlinear waveguide and consequently the parameters of the output multilens.

Therefore, the value of the beam width, peak displacement and wave number of the data wave without pump are now given by,

$$aw_{d0}(z_3) = \frac{2B}{k}\frac{1}{aw_{d0}(z_2)} = \frac{w_{d1}(z_2)w_g}{w_{d0}(z_2)}, \quad x_{d0}(z_3) = 0, \quad V_{d0}(z_3) = 0, \tag{30}$$

and the pump wave parameters at the plane z_3 are given are given by,

$$\begin{aligned} &aw_{p1}(z_3) = \frac{2B}{k}\frac{1}{aw_{p1}(z_2)} = \frac{w_{d1}(z_2)w_g}{w_{p1}(z_2)}, \quad x_{p1}(z_3) = \frac{B}{k}x_{p1}(z_2) = \frac{1}{2}aw_{d1}(z_2)w_g V_{p1}(z_2), \\ &V_{p1}(z_3) = -\frac{k}{B}x_{p1}(z_2) = \frac{2}{aw_{d1}(z_2)w_g}x_{p1}(z_2). \end{aligned} \tag{31}$$

By solving the system of equations (24), (25) and (26) for the quasi-selftrapping power for the pump wave, that is $p_{p1} = p_{st}$ (given by the equation (15)), we find the distance of propagation which makes sure the condition (29), that is $z_2 - z_1 = 25.84$ mm. Once the optimal distance value has been obtained, we calculate, from Eqs. (23), the values for the Gaussian parameters of the data beam in the absence of pump. In Fig. 8 are shown the plots derived from the results from the design, where it can be observed the quantitative evolution of the beams for each routing operation.

Let us evaluate the validity of the design by calculating the transverse modal coupling efficiency of the data and pump waves for each output optical fibers. For that, let us introduce first the expressions for the normalized amplitudes of the incoming Gaussian beams ψ_σ at the plane z_3 where the subindex σ gives account of the notation ($\sigma = d0, d1, p1$),

$$\psi_\sigma(x) = \frac{2^{1/4}}{(\pi a^2 w_\sigma^2)^{1/4}} \exp\left[-\frac{(x-x_\sigma)^2}{a^2 w_\sigma^2}\right] \exp\left[\mathrm{i}V_\sigma(x-x_\sigma)\right], \tag{32}$$

#6293 - $15.00 US Received 11 January 2005; revised 18 April 2005; accepted 19 April 2005

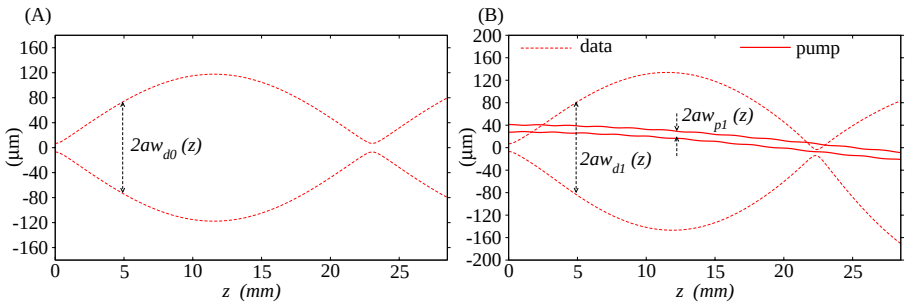

Fig. 8. Propagation plots (top view) for the data routing operation. (A) Data wave propagation under the absence of pump (header bit "0"); (B) Data and pump wave propagation under the presence of pump (header bit "1").

moreover, the Gaussian modal amplitude φ_f of an optical fiber displaced a value Δ respect to the x-axis, is expressed as follows,

$$\varphi_g(x) = \frac{2^{1/4}}{(\pi w_g^2)^{1/4}} \exp\left[-\frac{(x-\Delta)^2}{w_g^2}\right]. \tag{33}$$

The transverse modal coupling efficiency can be determined at z_3 by the following expression [22],

$$\eta_\sigma = \left|\int_{-\infty}^{\infty} \psi_\sigma(x)\varphi_g(x)\mathrm{d}x\right|^2 = \frac{2aw_\sigma w_g}{a^2w_\sigma^2 + w_g^2} \exp\left[-\frac{1}{2}\frac{a^2w_\sigma^2 w_g^2 V_\sigma^2 + 4(x_\sigma - \Delta)^2}{a^2w_\sigma^2 + w_g^2}\right], \tag{34}$$

where $\Delta = 0$ for fiber 1 and $\Delta = -\delta$ for fiber 2. Finally, these are the results for the transverse modal coupling on each fiber for the propagating waves in both operation states,

	η_{d0}	η_{d1}	η_{p1}
Fiber 1	0.900	1.20×10^{-11}	0.090
Fiber 2	6.50×10^{-7}	0.888	0.090

Table 1. Transverse coupling efficiencies of the data and pump beams onto the output optical fibers.

As the results show, the data packet is transmitted through each fiber with a high efficiency (higher than the 85 %) for each case; on the other hand, the most important result is that the cross-talk of the transmission is negligible since the coupling efficiencies of data packet on the non-corresponding channel are lower than 0.0001 %; in addition, the pump wave presents an optical coupling efficiency onto both channels about 10 %; although it is not negligible, it is enough to preserve the data packet free of nonlinear effects for further incorporation to cascaded devices.

7. Cascaded configuration for N-port routing.

The implementation of a single-bit routing module, presented above, routes the data signal onto two different output channels. It is the first step towards a general multi-port routing operation as a function of a generalized header composed by an array of bits. The header encoding in

#6293 - $15.00 US Received 11 January 2005; revised 18 April 2005; accepted 19 April 2005

a N-bit binary format, allows the routing of the data packet towards 2^N output ports, and the routing path must be determined by the header binary value.

In the Fig. 9 is shown a scheme of a 2-bit routing operation (the generalization to N-bit is intuitive by means of cascadability), where a 4-port routing configuration is presented for a generalized encoding of the header. The input packets are modulated with the same intensity values for the data and the header, presenting a realistic case of information encoding. The

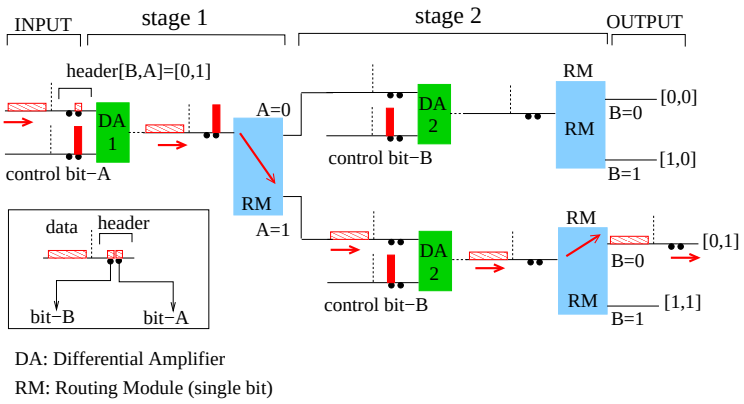

Fig. 9. Scheme of the cascaded configuration for multi-bit header routing where a [0,1] header routes the data packet onto its correspondent output channel.

previous step for the proposed routing strategy is to amplify the header bits in order to switch the data packet into its corresponding channel; for that, an all-optical Differential Amplifier (DA), which can be implemented under the same physical mechanism as the devices presented in this work (see reference [10]), is fed with a reference signal synchronized with the corresponding header bit in each stage (see Fig. 9). Therefore, in the first stage, the first header bit (bit-A) is amplified and the first single-bit Routing Module (RM) performs the corresponding routing operation where both the data packet and the non-amplified header bits are transmitted through the corresponding output channel. In the second stage, the 0-valued bit-B does not switch up the DA, and the second RM routes the data packet to the output channel labelled as [0,1] in Fig. 9. Finally, a whole routing process as a function of the binary value of the header N-bit array, can be performed by sequentially cascading the single bit routing stages onto each output of the RMs.

8. Conclusions

An integrated optical system has been fully designed for a phase-insensitive all-optical routing operation. By means of the variational method, we have obtained the evolution equations for the characteristic parameters of single, co- and counter-propagating Gaussian beams in a nonlinear lenslike waveguide. Starting from these results and in connection with the theory and design of integrated waveguiding multilenses, three integrated all-optical devices devoted to header bit extraction, bistability and data routing, have been designed under a unique technology. The optical system proposed shows a robust, phase-insensitive and fiber compatible single-bit routing operation. Finally, by connecting several integrated optical systems of this kind in a cascaded way a N-bit router can be implemented.

#6293 - $15.00 US
Received 11 January 2005; revised 18 April 2005; accepted 19 April 2005

Acknowledgments

This work was supported by contract TIC2003-08992, Ministerio de Ciencia y Tecnología (Spain).

Appendix

In this work the design of the integrated multilens is based on one or two modules performing, each one of them, an Exact Fourier Transform (EFT) of the input beam. The configuration, for instance, of a multilens with two modules and their characteristic parameters are shown in Fig.10.

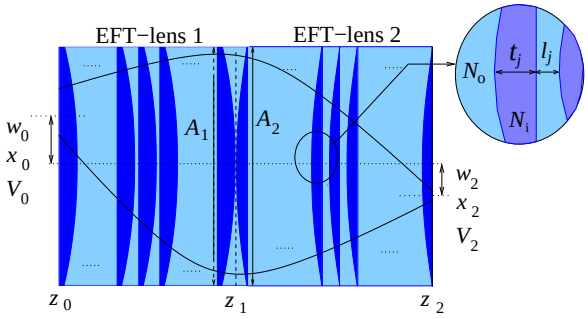

Fig. 10. Sketch of a multilens with two EFT modules.

Let us define each EFT module $j = 1,2$ as a planar integrated multilens composed by m_j plane-convex lenses of thickness t_j and aperture A_j separated a distance l_j with effective indexes N_i and N_o inside and outside of each lens. It can be demonstrated (explicit calculus is found in reference [17]) that each module j produces, at z_j-planes, an Exact Fourier Transform of the Gaussian beam at z_{j-1}-planes if the following conditions are fulfilled,

$$N_o t_j = N_i l_j, \qquad m_j \cos^{-1}\left(1 - \frac{t_j}{N_i f_j}\right) = \frac{\pi}{2}, \tag{A.1}$$

where f_j are the focal lengths of each plane-convex lens, that is:

$$f_j = \frac{N_o}{N_i - N_o}\frac{1}{t_j}\left[t_j^2 + (A_j/2)^2\right]. \tag{A.2}$$

Now, by defining the Gaussian beam width, peak displacement and wave number at planes z_j (see Fig.10) as w_j, x_j and V_j respectively, the following relationships, for a single EFT module, are obtained for the transformation of the beam parameters:

$$aw_j = \frac{2B_j}{k}\frac{1}{aw_{j-1}}, \quad x_j = \frac{B_j}{k}V_{j-1} \quad \text{and} \quad V_j = -\frac{k}{B_j}x_{j-1}, \tag{A.3}$$

where,

$$B_j = \left[\frac{2t_j f_j}{N_i} - \frac{t_j^2}{N_o^2}\right]. \tag{A.4}$$

Finally, by combining the expressions (A.3) it can be easily obtained the following relationships for two EFT modules, that is:

$$aw_2 = \frac{B_2}{B_1}aw_0, \quad x_2 = -\frac{B_2}{B_1}x_0 \quad \text{and} \quad V_2 = -\frac{B_1}{B_2}V_0. \tag{A.5}$$

#6293 - $15.00 US Received 11 January 2005; revised 18 April 2005; accepted 19 April 2005